NMR IMAGING OF SNOW

Toshihiro Ozeki*
Ship Research Institute, Mitaka, Japan
Akihiro Hachikubo
Kitami Institute of Technology, Kitami, Japan
Katsumi Kose
Institute of Applied Physics, University of Tsukuba, Tsukuba, Japan
Kouichi Nishimura
Institute of Low Temperature Science, Hokkaido University, Sapporo, Japan

ABSTRACT: NMR imaging was introduced to visualize and analyze the three-dimensional structure of snowpack. We used three types of snow; ice spheres, coarsened snow grains and depth-hoar crystals. In particular, because ice spheres had a uniform particle size and large enough, they was suitable material for the test imaging. Because the NMR signal from the ice was very weak, the air space of snow was filled with iron-acetylaetonate doped dodecane $C_{12}H_{26}$, which had a good infiltration property and a low freezing point (about -12 °C), and we looked at the space occupied with dodecane instead. The result of test imaging of Dodecane showed 0.5 to 2 hours were needed to obtain the one 3D image, and hence we developed a specimen-cooling system using nested pipes. Cold air was sent between the pipes to keep the temperature below 0 °C. Experiments using the above snow and the system were carried out and we succeeded to obtain 3D microscopic images; the image matrix was 128^3 and voxel size was 0.2 mm^3.

KEYWORD: NMR, three-dimensional imaging, snow structure, ice sphere, dodecane

1. INTRODUCTUION

Microstructure of the snowpack should be better understood because it affects the mechanical and physical properties of snow; for instance, heat conduction and shear strength; and also affects the optical properties. The avalanche release mechanism also depends on the snowpack's microstructure. Thin sections and plane-surface sections are currently used to investigate the microstructure of the snowpack. However, they have only two-dimensional information; therefore, a large number of operations are necessary to reconstruct the three-dimensional structure using stereological methods. Several groups are now developing new methods to get the 3D microstructure of snow (Coléou *et. al.*, 2000; Schneebeli and Krüsi, 2000). Instead of the latter techniques, we have developed a nuclear magnetic resonance (NMR) imaging technique to visualize the 3D structure of snowpack.

Nuclear magnetic resonance imaging, which coupled with the explosive growth of digital computers, is playing an important role in medical imaging over the last several years. Magnetic resonance imaging has advanced as a tomographic technique to produce images of the inside of the human body. Fat and water, which primarily make up the human body, have many hydrogen atoms. MRI images an NMR signal from the hydrogen nuclei. Therefore development of NMR imaging has enhanced our ability to diagnose and monitor diseases. Because NMR is particularly sensitive to the proton magnetic moment of water and organic compounds, Edelstein and Schulson (1991) applied NMR imaging to visualize drainage channels within salt-water ice. Manfres *et. al.* (2000) used NMR to visualize oil diffusion into sea ice. Although there have been several studies on NMR imaging of sea ice, there have been few attempts to use NMR to visualize snowpack. In this study, an NMR imaging system with a small temperature-controlled chamber was developed, and then used to visualize snowpack samples.

2. MATERIALS AND METHODS

In the imaging of snowpack, the NMR signal from the ice was very weak. For this

* *Corresponding author address:*
Toshihiro Ozeki, Hokkaido University of Education, Iwamizawa, Hokkaido 068-8642, JAPAN; tel & fax: +81-126-32-0336;
email: oze@iwa.hokkyodai.ac.jp

reason, the air spaces in the snow was filled with dodecane doped with iron acetylaetonate $C_{12}H_{26}$, which has a good infiltration property and a low freezing point (about -12 °C). Thus, the NMR imaged the space occupied with dodecane instead of ice particles.

The three-dimensional microscopic images, which have 128^3 pixcels, were obtained with a homebuilt NMR imaging system (Kose, 1996) using a 4.74-T, 89-mm vertical-bore superconducting magnet (Oxford Instruments) and an actively-shielded gradient coil (Doty Scientific). The apparatus is shown in Fig. 1. The phase-encoding directions are the x and y directions, and the signal readout direction is the z direction.

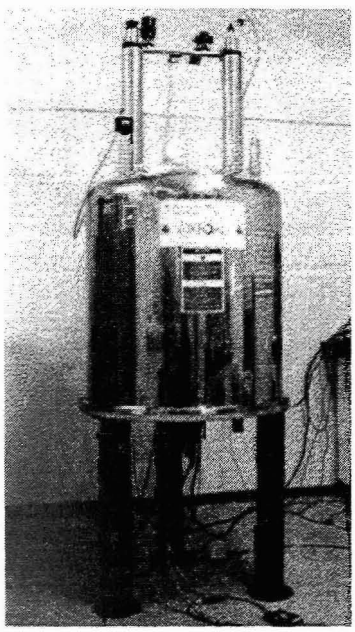

Fig. 1: Superconducting magnet of our homebuilt MRI system.

The intensity of the NMR signal was first tested using nylon spheres of 3.2-mm diameter instead of ice particles, and then we filled the interstitial pores with dodecane. Fig. 2 shows a 0.2-mm slice of the complete 3D microscopic image; this 2D image had a pixel size of 0.2x0.2 mm^2. The measurement time for one 3D image was 30 minutes. Because the nylon spheres did not have an NMR signal, the nylon spheres image as dark disks. This test shows that dodecane provides enough signal to distinguish dodecane from the nylon spheres, although it was necessary to improve the signal to noise ratio.

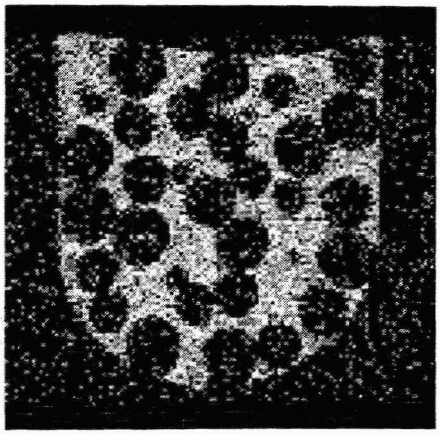

Fig. 2: 2D NMR image of nylon spheres in dodecane.

Because signal accumulations were done to reduce the noise, the total measurement time for one 3D image was 30 to 60 minutes. As this measurement time is long, we developed a specimen-cooling system to keep the temperature below 0 °C. This system has a double-pipe cylinder made of acrylic plastic with outer diameter of 40 mm and inner diameter of 20 mm through which cold air was passed.

Three types of snow were prepared for the NMR imaging: ice spheres of about 3-mm diameter, coarsened snow grains, and depth-hoar crystals. In particular, because ice spheres are sufficiently large and uniformly sized, they were ideal for test imaging.

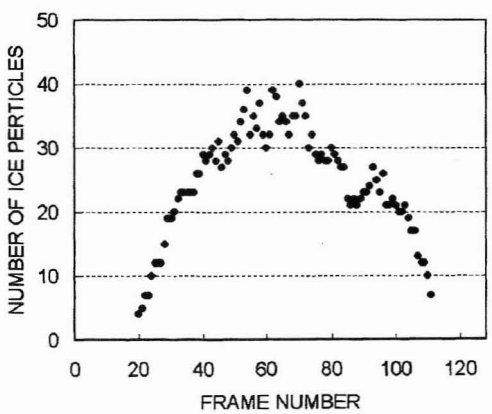

Fig. 3: Number of ice particles in each frame.

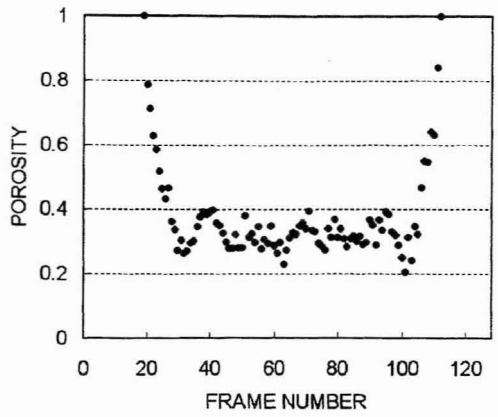

Fig. 4: Porosity distribution.

3. EXPERIMENTAL RESULTS

Fig. 3 shows number of ice spheres in each frame (0.2-mm thick slice) of the 3D data. The abscissa indicates the frame number from 1 to 128. The signal of dodecane appeared from the 19th frame to the 112th frame. The number of ice particles is distributed nearly symmetrically in a bell-like curve with a peak between the 60th and 70th frames. This distribution is primarily due to the variable cross-sectional area of our cylindrical sample holder. This is supported by the nearly uniform porosity distribution that is plotted in Fig. 4. In this study, porosity was defined as the ratio of the dodecane area (bright area) to the whole sample area in one cross-sectional image. An edge effect of the sample holder is shown on both sides of the plots; the thickness of this edge region is approximately the diameter of the ice spheres. Although there are fluctuations, the porosity is nearly uniform between the 30th and 100th frames: the average is 0.32 and the standard deviation is 0.04. This value is almost the same as the porosity of closest packing of spheres (0.26).

Fig. 5 shows 2D cross-sectional slices of the 3D image data of ice spheres; of the 128 slices that complete the sample, (A) is the 43rd, (B) the 45th, and (C) the 51st frame. There is a gap of 0.2 mm between A and B, and C is the frame 1 mm from B. Because we could measure the NMR signal from dodecane, but not from the ice spheres, the ice spheres appear as dark disks or semicircles. The arrows in each frame indicate how the diameter of the same ice spheres change with frame change. The dark disks first appear, grow, and later disappear as we step through the sequence of frames.

Fig. 6 illustrates a volume-rendered 3D display of ice spheres. Because the NMR signal was obtained from dodecane, this is the negative image of ice spheres; *i.e.*, ice spheres are reconstructed as cavities. Negative images of the above 3D data were processed to visualize ice spheres; this image-processed 3D display is shown in Fig. 7. This figure illustrates not only the volume-rendered 3D image, but also a cross-sectional image on the front side. As shown in Fig. 7, we can see the 3D structure of packed ice spheres by viewing such displays from various angles and cross sections.

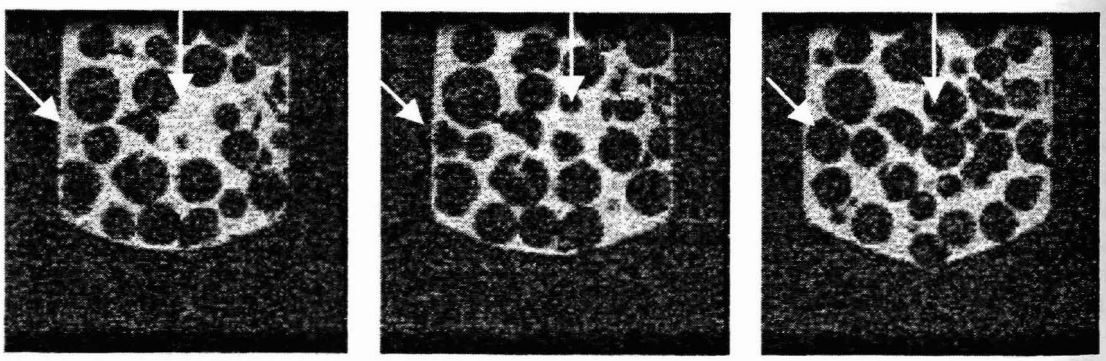

(A) 43 / 128 (B) 45 / 128 (C) 51 / 128

Fig. 5: 2D cross-sectional images from the 3D image of ice spheres.
A, B, and C are the 43rd, 45th, and 51st cross sections, respectively.

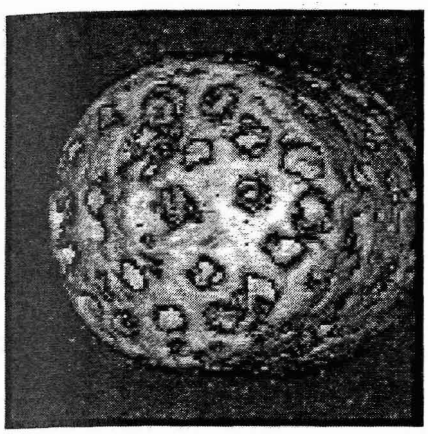

Fig. 6: Volume-rendered 3D display of ice spheres (reversed image).

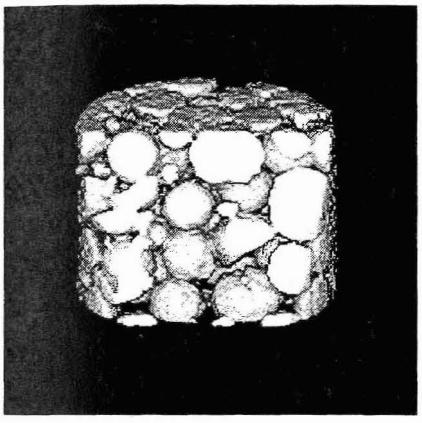

Fig. 7: Negative black-white image of ice spheres in dodecane.

Fig. 8 shows a cross sectional image of depth-hoar crystal with dodecane. Since the depth-hoar layer was disassembled to pack into the sample holder, the depth-hoar sample didn't keep the original structure. The depth-hoar crystals were solid or striated plates, and hence we can see the negative image of the depth-hoar as dark lines in the cross-section. Because the efficiency of the cooling system was reduced by frost condensation, signal accumulation time of coarsened snow grains was not enough, and the 3D data was noisy.

Continuous measurements during melting of the ice spheres was carried out, and 3D microscopic images were obtained 17 times in 110 minutes; the image matrix is 64^3 and the voxel size is 0.4 mm^3. Fig. 9 shows the same slice for the 3rd (A), 6th (B), and the 15th (C) image of the 17 3D data sets. In this series, conductive heat from the cylinder pipe raised the temperature of the sample with time. Because the ice spheres and the dodecane were frozen in Fig. 9 (A), the NMR signals were very weak and the entire image is dark. On the other hand, Fig. 9 (B) shows a suitable condition for NMR imaging of snow; *i.e.*, the dodecane has melted and the ice spheres are still frozen. In Fig. 9 (C), heat conduction has melted the ice spheres near the pipe and the melt water has an NMR signal as well as the dodecane. These results show that NMR imaging is useful for continuous, non-destructive measurements, and could be a powerful technique to study the structure of snowpack.

4. CONCLUSIONS

NMR imaging was introduced to visualize the three-dimensional structure of snowpack. Because the NMR signal from the ice was very weak, the air space in the snow was filled with dodecane, and we imaged the space occupied by dodecane instead. Because 0.5 to 2 hours were needed to obtain one 3D image of dodecane, a specimen-cooling system was developed that consisted of nested pipes. We obtained 3D microscopic images using ice spheres, depth-hoar crystals with a voxel size of 0.2 mm^3. This NMR imaging method of snow with dodecane appears to be a superb way to visualize the structure inside snowpack. We can see the 3D structure of a bed of ice spheres by viewing 3D displays from various angles and cross sections. Also, continuous measurements during the melting of snow showed that NMR imaging is useful because it is non-destructive. In future experiments, we expect to see not only the melting, but also the growing and breaking of snow. Although it is necessary to improve the resolution and to reduce the noise, we expect that shortening dodecane's relaxation time of will allow these improvements, and thus we expect that the 3D network of a snowpack will be shown clearly soon.

ACKNOWLEDGEMENTS

We are grateful to Mr. S. Nakatsubo of Institute of Low Temperature Science, Hokkaido University for his work in assembling and operating the specimen-cooling system.

We also thank Mr. T. Haishi of Institute of Applied Physics, University of Tsukuba for his work in operating the NMR imaging system.

5. REFERENCE

Coléou C., B. Lesaffre, J. B. Brzoska, W. Ludwig, E. Boller, 2000. 3-D snow images by X-rays micro-tomography. Abstracts of Int. Sym. Snow, Avalanches and Imp. Forest Cover, paper No. 64.

Edelstein, W. A., E. M. Schulson, 1991. NMR imaging of salt-water ice. J. Glaciol. 37, 177-180.

Kose, K., 1996. 3D NMR imaging of foam structures. J. Mag. Resonance A118, 195-201.

Manfred. A., U. Buschmann, B. Pfleiderer, 2000. Oil and Sea Ice : NMR Tomography. Abstracts of Int. Sym. Sea Ice and Its Interactions, paper No. 33A202.

Schneebeli, M. and G. Krüsi, 2000. Three-dimensional reconstruction of snow. Abstracts of Int. Sym. Snow, Avalanches and Imp. Forest Cover, paper No. 97.

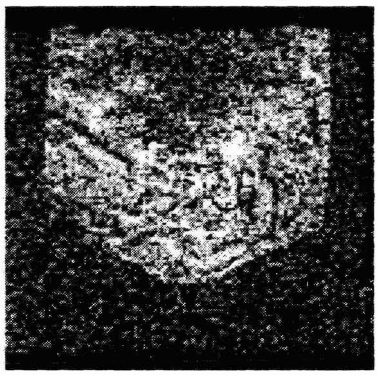

Fig 8: 2D cross-sectional image of depth-hoar crystals.

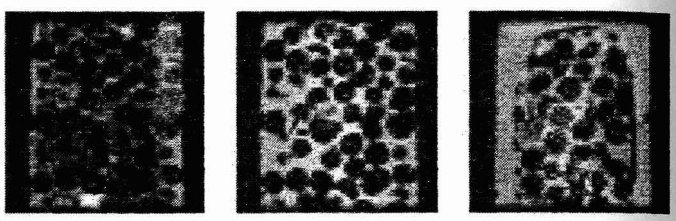

(A) 3 / 17 (B) 6 / 17 (C) 15 / 17

Fig 9: 2D cross-sectional images of ice spheres during melting. (A) Dodecane and ice are frozen, (B) Dodecane melted with ice frozen, and (C) Ice spheres are melting.